CHAPTER 4

GROWTH AND CHARACTERIZATION OF THE $MoSe_xTe_{2-x}$ SINGLE CRYSTALS

CONTENTS

4.1 Introduction

It has already been seen that transition metal dichalcogenides, are considerably important because of their usefulness as lubricating materials, switching devices, electrodes for photoelectrochemical solar cells, etc. The chemical vapour transport techniques, described in the earlier chapter, using halogen (Br or I) as the transporting agent has been found to be a suitable technique by several workers[1-7] for growing the single crystals of layered compounds. It appears from the literature that there has been no previous attempt to grow the single crystals of $MoSe_xTe_{2-x}$ ($0 \leq x \leq 2$). Kline et al[8] reported that the transition metal dichalcogenides (TMDC) form a wide range of solid solutions[9,10] with either mixed metal or chalcogenide composition or both and the properties, like crystal structure, band gap, band positions and stability to corrosion, which are of prime interest to photoelectrochemist might be influenced by changing the composition of the layered crystals. In present chapter author

reports the growth and characterization of $MoSe_xTe_{2-x}$ ($0 \leq x \leq 2$) single crystals.

4.2 Experimental

Stoichiometric amounts of 99.999 % pure molybdenum, selenium and tellurium were introduced into a cleaned, etched and vacuum backed quartz ampoule of internal diameter 25 mm and length 200 mm. A total charge of about 9-12 gm was used in the experiment. A weight ρ (3 mg/cm^3 to 4 mg/cm^3 of ampoules volume) of liquid bromine was introduced into the ampoule in a sealed capillary tube. The ampoule was then evacuated to a pressure less than 10^{-5} torr and sealed at the constriction 3 mm in diameter.

The ampoule was vigorously vibrated to ensure that the capillary tube breaks releasing the bromine and the powders were mixed properly. The mixture was distributed along the length of the ampoule and placed in a two-zone horizontal furnace and the temperature was slowly increased to $700^{\circ}C$ in the manner described in the earlier chapter. The ampoule was left at this temperature for 72 hours.

Then the furnace was shut down and allowed to cool down to room temperature. A free flowing shinning dark mixture resulted from the reaction.

4.3 Growth of Single Crystals

The charge thus prepared was well mixed by vigorous shaking of the ampoule. The powder was then distributed along the length of the ampoule and the ampoules was kept in the furnace again for the growth of crystals as shown in Fig. 4.1. The furnace temperature was increased slowly, as was done for charge preparation, to the required final temperature for growth.

The exact growth conditions adopted for different compositions have been described in Table 4.1. Figure 4.2 shows in general the temperature gradient maintained along the ampoule. After the required period of growth the furnace was shut off and allowed to cool down to room temperature. The ampoule was broken and crystals were found to be grown.

The crystals obtained are grey-black, in

Table 4.1

Growth conditions used to produce single crystals of $MoSe_xTe_{2-x}$

Nominal Composition x	Reaction temperature (°C)	Growth temperature (°C)	Growth time (h)
$MoTe_2$ 0.0	700	650	72
0.5	900	800	48
1.0	800	670	96
1.5	880	720	168
$MoSe_2$ 2.0	900	800	120

colour and plate-like with the c-axis normal to the plane of the plates and all of them grew over the transported charge inside the ampoule.

4.4 Structure

The system $MoSe_xTe_{2-x}$ (0 x 2) is simple because both the end members $MoSe_2$ and $MoTe_2$ as well as the intermediate members have the same MoS_2 structure (C_7 type) as indicated by Champion[11]. The basic co-ordination unit for these structures is trigonal prismatic. A S-Mo-S sandwitch layer is composed of alternately occupied, face-shared prisms, the Mo and S atoms forming close packed layers. No strong bond exists between the layers, only long-range Van der Waal's forces hold atomic sandwitches together. This gives the crystals their characteristic platy habit, with extended growth and pronounced cleavage perpendicular to C-axis. The stacking sequence is AbABab, where S stacking is represented by capital letters, with the space group D^4_{6h} ($P6_3/mmc$).

4.5 Determinationof Lattice Parameters

X-ray diffraction technique are useful

tools for structural investigations. These techniques, based on monochromatic radiation, are important because the d-spacings can be calculated from the observed diffraction angles. In diffractometer, the diffracted radiation is detected by a counter tube which moves through an angular range of reflections. The intensities are recorded on synchronously advancing strip-charts.

The Bragg-Brentano X-ray diffractometer, shown in Fig. 4.3 is used in the present work. Here the specimen is mounted at the centre of the diffractometer and rotated by an angle θ around an axis in the specimen plane. The counter is attached to an arm rotating around the same axis by angles twice as large as those of the specimen rotation. Only (hkl) planes parallel to specimen plane contribute to the diffracted intensity.

X-ray diffractometer traces obtained using the diffractometer above, were used to determine the unit cell dimensions as depicted in Fig. 4.4. The values of lattice parameters 'a' and 'c' determined

from the analysis of these traces have been given in Table 4.2. The compositional dependence of lattice parameters and X-ray density are plotted in Fig. 4.5. The 'a' parameter varies linearly with composition according to equation (4.1).

$$a(X) = (3.530 - 0.247\ X)\ A^{o} \qquad (4.1)$$

where 'x' defines the solid solution $MoSe_xTe_{2-x}$. Variation of the C-parameter is also linear and is given in equation (4.2).

$$c(X) = (13.882 - 0.310\ X)\ A^{o} \qquad (4.2)$$

Densities have been calculated from unit cell dimensions for all compositions. Values of density and c/a ratio are listed in Table 4.2. The density also follows a linear variation Fig. 4.5 of the form,

$$D(X) = (7.805 - 0.32\ X\ )\ A^{o} \qquad (4.3)$$

Table 4.2

Lattice parameters, c/a ratio and calculated density for layered compounds in the series $MoSe_2Te_{2-x}$

Nominal composition x	a (nm)	c (nm)	c/a	Calculated density ($g\ cm^{-2}$)
0.0	0.3530 ± 0.002	1.3882 ± 0.004	3.917	7.805
0.5	0.3456 ± 0.008	1.3736 ± 0.020	3.974	7.638
1.0	0.3396 ± 00.010	1.3510 ± 0.010	3.978	7.450
1.5	0.3376 ± 0.001	1.3146 ± 0.006	3.939	7.299
2.0	0.3283	1.2918	3.935	7.004

The series of layer compounds form a complete range of isomorphous solid solutions.

4.6 Energy Dispersive X-ray Analysis (EDAX)

Some of the signals which can be detected contain specific chemical information. Principal among these are the characteristic X-ray photographs which have been the basis of electron microprobe analysis for more than 25 years. During the last nine years the situation has been radically changed by the commercial availability of energy dispersive X-ray analysis systems (EDAX) which detect individual X-ray photons. The spectrum obtained by these systems is a "finger-print" of the chemical content of the sample. The combination of SEM and EDAX is an extremely powerful general purpose instrument, especially since regions of X-ray spectrum can be selected to form a distribution map of any desired element.

When a beam of electrons strikes a specimen, a fraction of the incident electrons excite

the atoms of the specimen which then emit X-rays when they return to their ground state. The energy of these X-rays is strictly characteristic of the atomic number of the elements excited and therefore their detection forms the basis of elemental analysis in the electron microscope (Fig. 4.6). The X-ray thus generated are detected usually by a solid state detector (A lithium drifted silicon p-i-n diode held at liquid nitrogen temperature has been used as the detector in the Philips EM 400 used in the present study). A beryllium window covers the cooled detector. The output pulses are stored in a multi-channel analyser. The analysis of the spectrum has been done by energy dispersion. Elements from sodium upwards in the periodic table, can be detected by this technique.

For quantitative microprobe analysis the incident electrn probe is maintained stationary in the appropriate area while an X-ray spectrum is being collected. The characteristic peaks in this spectrum have been used to identify the constituents of the specimen and the various X-ray relative intensities have been used for quantitative analysis. However, for

an accuracy of a few percent, the method requires the use of elemental standards and a number of corrections are to be applied in the final composition.

Only a semi quantitative analysis of the crystals has been done in the present study. As the samples were neither bulk nor thin i.e. partially transmitting, the electron beam, ZAF correction was not applied to the results.

The weight percentages of molybdenum, selenium and tellurium in different crystals of $MoSe_xTe_{2-x}$ determined from the EDAX are given in Table 4.3.

4.7 Microstructure

A large number of experimental and theoretical studies[12-20] have been done to understand the crystal growth mechanisms. Microtopographical studies of the as-grown faces is one of the methods by which an understanding of the crystal growth and dissolution can be made, mainly because of the fact that habit faces exhibit growth features.

Table 4.3

Weight percentage of layer compounds in the series $MoSe_xTe_{2-x}$ obtained by EDAX

Nominal composition x		wt % of elements present		
		Mo	Se	Te
$MoTe_2$	0.0	22.155	-	74.174
	0.5	24.786	28.984	45.958
	1.0	25.743	40.067	34.189
	1.5	33.975	54.717	11.307
$MoSe_2$	2.0	40.521	59.479	-

According to Frank's theory[14], thin platelets of basic structures form first by surface nucleation and layer by layer growth takes place under conditions of supersaturation. The crystallites formed at this stage may be perfect or they may contain twins or stacking faults on account of thermodynamic fluctuations during growth. As supersaturation drops below the critical value, the crystal platelets can only thicken further by the addition of material to self-perpetuating steps formed at the site of screw dislocation which may be originated by a buckle--followed up-slip mechanism as suggested by Frank[14]. As growth proceeds, these steps rotate around the center of the dislocation, finally creating a spiral as shown in Fig. 4.7.

It is well known[12] from the theory of crystal growth that the corners and edges of the crystals can serve as initiation points for the growth layers. In addition to the edges and corners of the crystals, certain impurities present on the crystal surface also serve as nucleation center for the growth layers.

One of the most striking features of layered crystals is the existence of screw dislocations with Burger's vector perpendicular to the plane of layers giving rise to the growth spirals. Different types of spirals are observed during present studies on microstructure. The surface microstructure on a typical MoSeTe single crystal as observed with scanning electron microscope (Philips EM 400) is shown in Fig. 4.8. This photograph reveals the presence of a hexagonal spiral suggesting thereby a screw dislocation mechanism of the growth for these crystals.

4.8 Conclusions

1. Single crystals of $MoSe_xTe_{2-x}$ have been grown by the chemical vapour transport technique because it yields large single crystals with relative ease.

2. The crystals are strain-free because they grow vertically in the form of thin platelets directly above the transported charge.

3. X-ray diffraction studies of the series indicate that all solutions formed are single

phase compounds, isomorphous with end members $MoSe_2$ and $MoTe_2$ with MoS_2 type structure.

4. The lattice parameters vary linearly with X.

5. The presence of hexagonal spirals on the faces of the grown crystals suggests a screw dislocation mechanism of growth for these crystals.

REFERENCES

1. Nitsche, R. (1960)
   J. Phys. Chem. Solids, 17, 163

2. Nitsche, R., Bolsterl , H. U. and
   Lichtensteiger, M. (1961)
   J. Phys. Chem. Solids, 21, 199.

3. Brixner, L. H. (1962)
   J. Inorg. Nucl. Chem., 24, 257.

4. Schafer, H. (1964)
   "Chemical Transport Reactions"
   (Academic Press, New York).

5. Nitsche, R. (1967)
   (Proceedings of an International
   Conference on Crystal Growth, Boston,
   1966).
   J. Phys.Chem. Solids, Suppl. No. 1, 215.

6. Nitsche, R. (1967)
   Crystal Growth, Ed. H.S. Peiser
   (Pergamon, Oxford) P. 215.

7. Al-Hilli, A. A. and Evans, B. L. (1972)
   J. Crystal Growth, 15, 93.

8. Kline, G., Kam,K. K., Ziegler, R. and Parkinson (1982) Solar Energy Materials, 6, 337.

9. Mentezen, B. F. and Sienko, M. J. (1976) Inorg. N Chem., 15, 2198.

10. Schneemeyer, L. F. and Sienko, M. J. (1980) Inorg. Chem., 19, 789.

11. Champion, J. A. (1965) British J. Appl. Phys., 16, 1035.

12. Chase, A. B. (1963) J. Am. Chem. Soc. 51, 107.

13. Gruber, E. E. and Mullins, W. W. (1967) J. Phys. Chem. Solids, 28, 875.

14. Frank, F. C. (1951) Phil. Mag., 42, 1014.

15. Cabrera, N. and Levine, M. M. (1956) Phil. Mag., 1, 450.

16. Burton, W. K., Cabrera, N. and Frank, F. C. (1951) Phil. Trans. Roy. Soc. London, A 243, 229.

17. Verma, A. R. (1953)
"Crystal Growth and Dislocations"
Butterworths, London.

18. Sunagawa, I. and Bennama, P. (1981)
J. Crystal Growth, 53, 490.

19. Sunagawa, I., Narita, K., Bennama, P.
and Vanderhock, B. (1977)
J. Crystal Growth, 42, 121.

20. Mitchel, R. S., Fujiki, Y. and
Ishizowa, Y. (1982)
J. Crystal Growth, 57, 273.

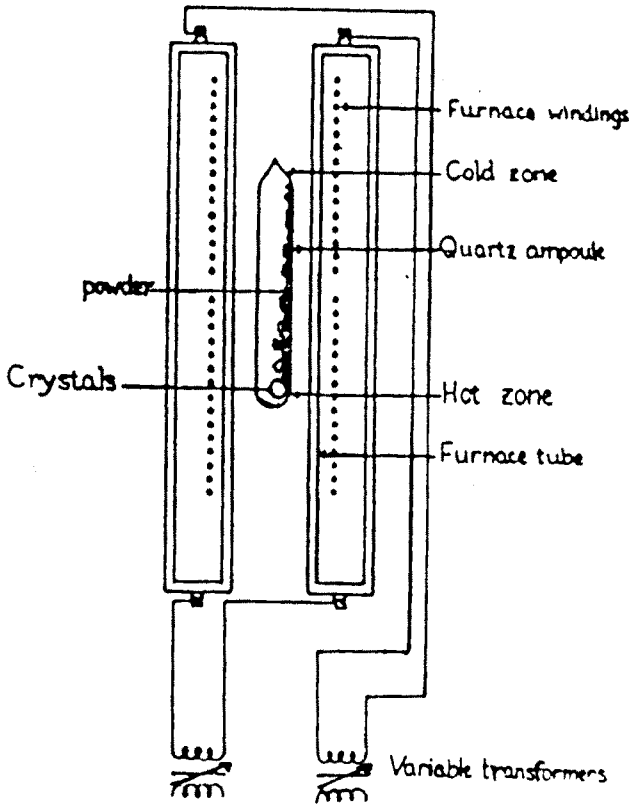

Fig. 4.1 Schematic view of the furnace showing the position of ampoule inside the two zone furnace during crystal growth

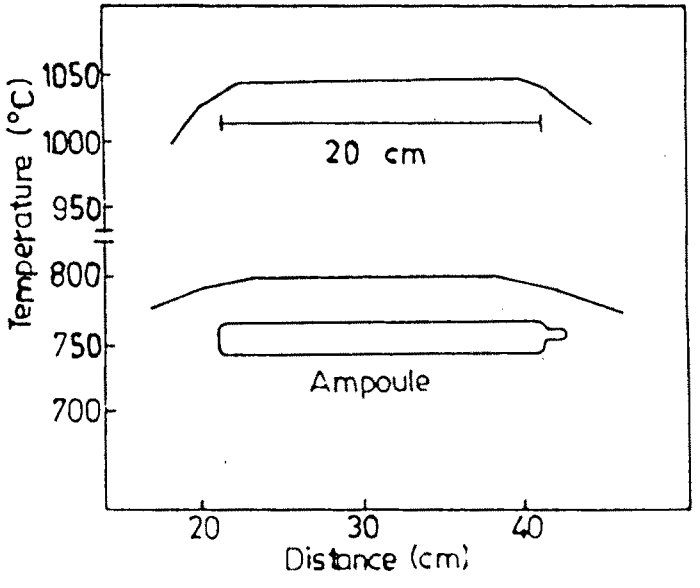

Fig. 4.2 Temperature profile of the furnace

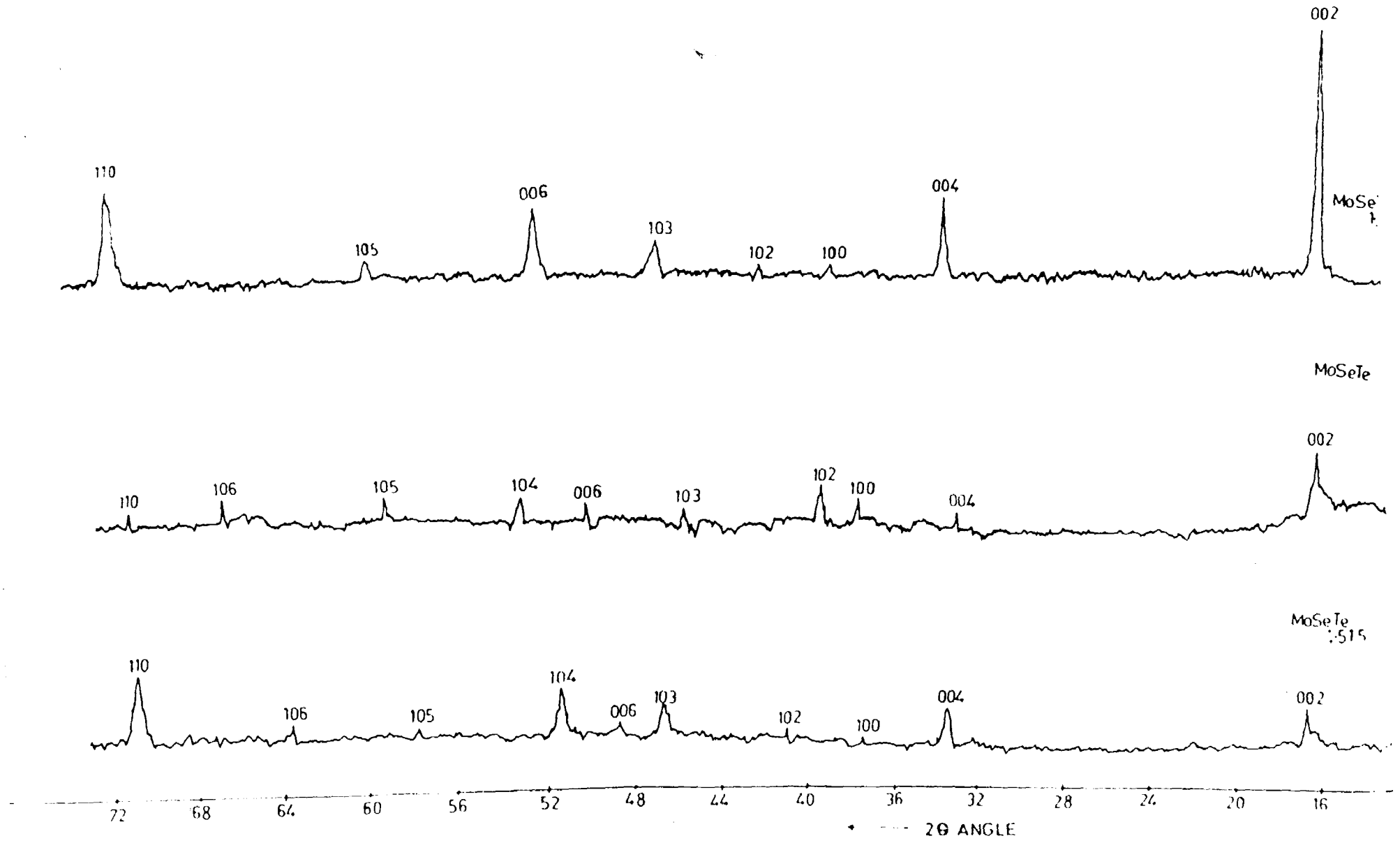

Fig. 4.4 X-ray diffractometer traces for $MoSe_{0.5}Te_{1.5}$, MoSeTe and $MoSe_{1.5}Te_{0.5}$ single crystals

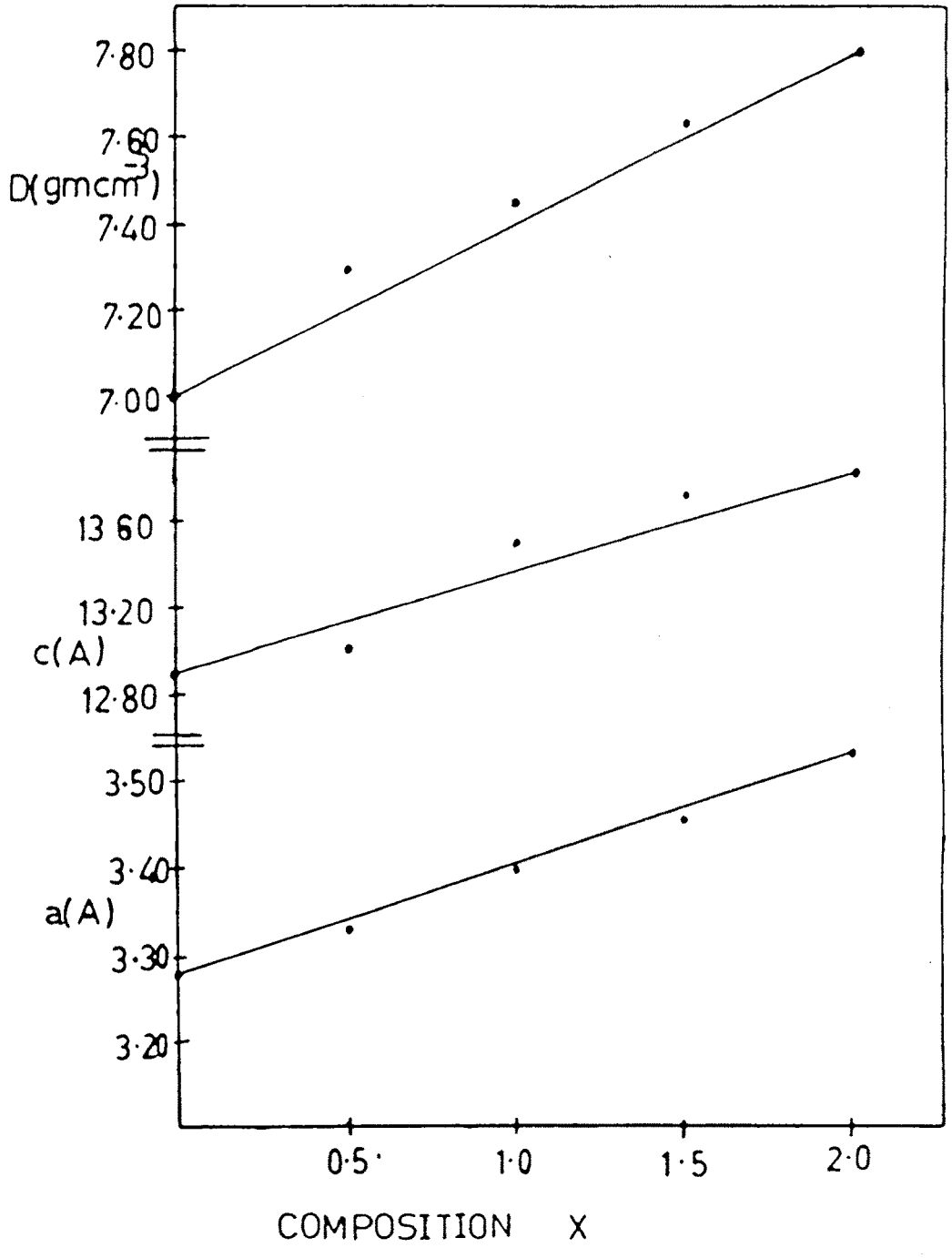

Fig. 4.5 Variation of 'a' and 'c' parameters and the X-ray density with composition

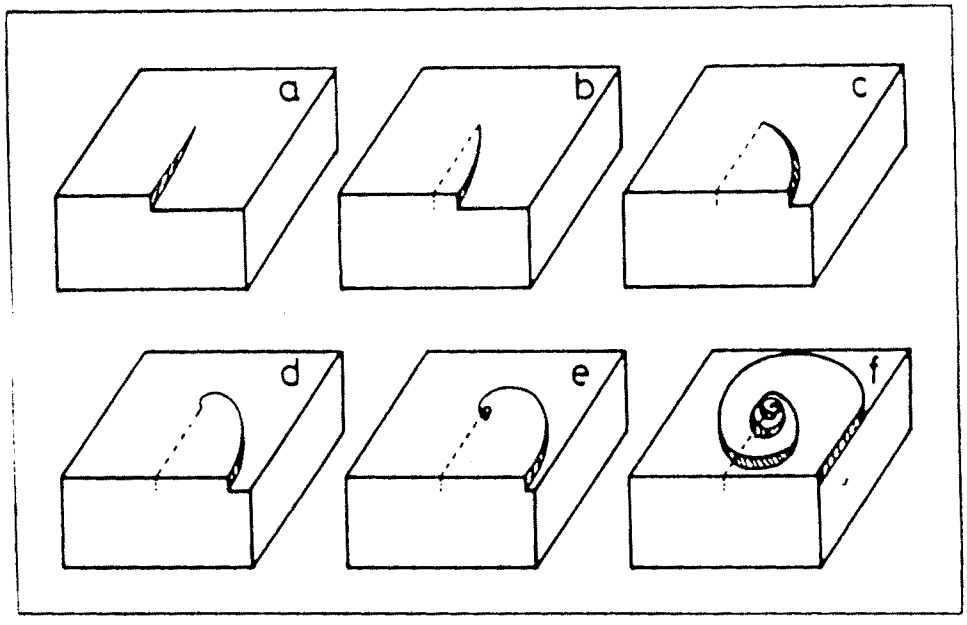

Fig. 4.7 Different stages of formation of spiral at a screw dislocation.

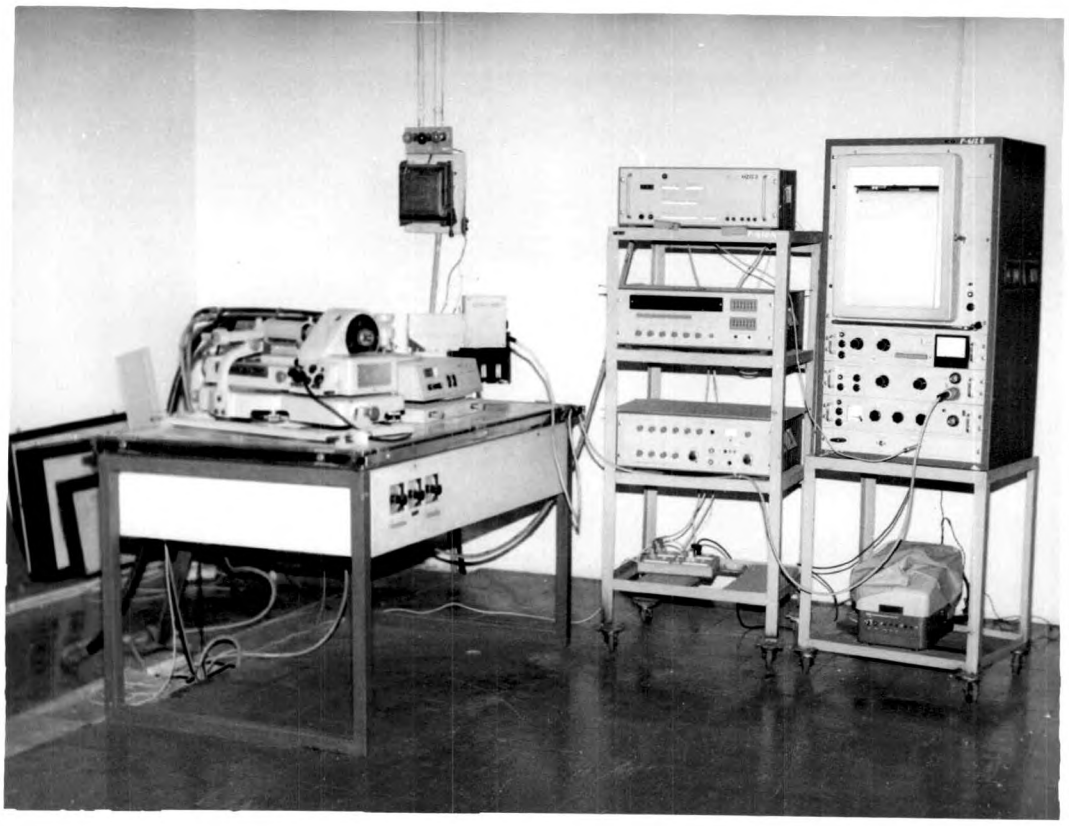

Fig. 4.3 The Bragg-Brentano X-ray diffractometer

Fig. 4.6 Philips EM 400

Electron Optical Microscope

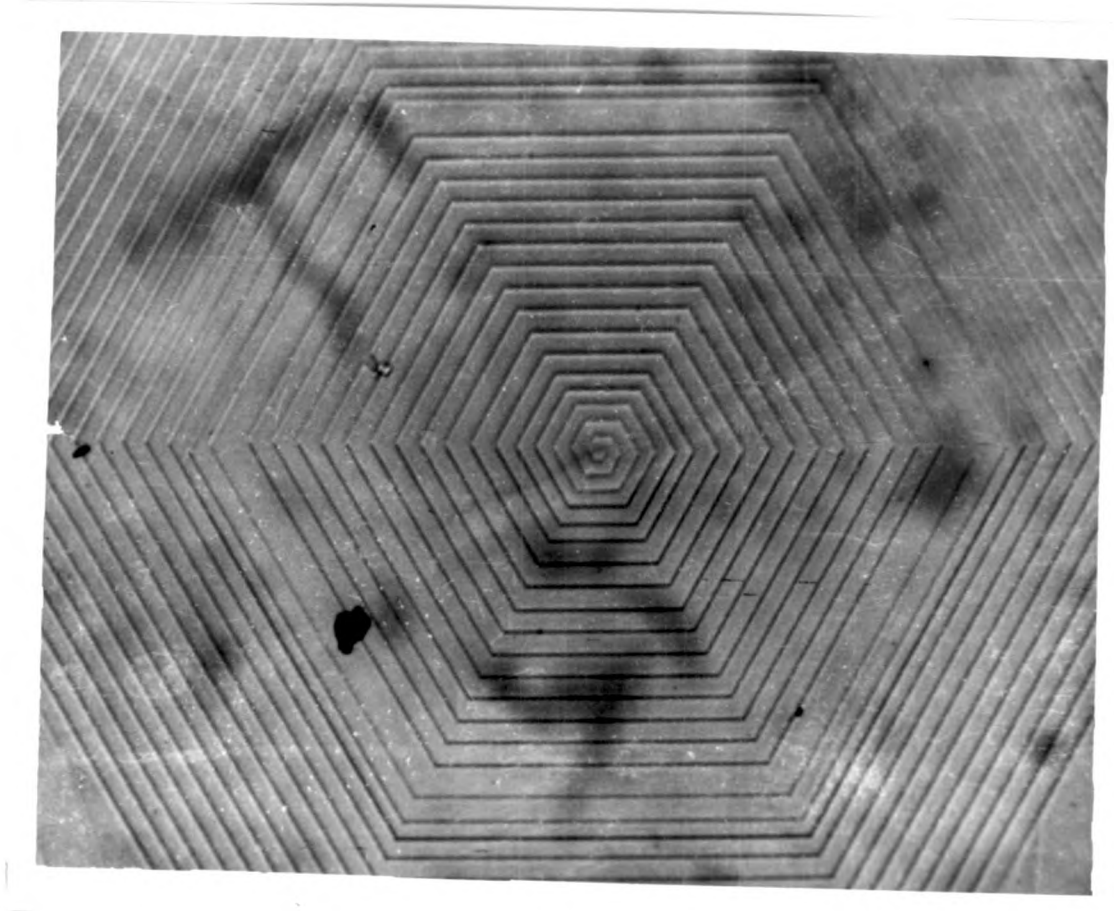

Fig. 4.8 Surface microstructure observed on the face of a typical MoSeTe crystals.